

## THE VALUE OF ULTRASOUND IN PREDICTION BREAST CANCER MOLECULAR SUBTYPES

Tran Thi Hue<sup>1,2</sup>, Dang Thi Hanh<sup>2,3</sup>, Le Thi Mai Huong<sup>2</sup>, Nguyen Van Tuan<sup>4</sup>,  
 Nguyen Thu Huong<sup>1</sup>, Nguyen Duy Hung<sup>2,5</sup>, Nguyen Minh Duc<sup>6</sup>

1 – Breast center, Vinmec Times City International Hospital. Ha Noi, Viet Nam.

2 – Department of Radiology, Hanoi Medical University. Ha Noi, Viet Nam.

3 – Department of Radiology, Ha Dong General Hospital. Ha Noi, Viet Nam.

4 – Radiology Center, Hanoi Medical University Hospital. Hanoi, Vietnam.

5 – Department of Radiology, Viet Duc Hospital. Ha Noi, Viet Nam.

6 – Department of Radiology, Pham Ngoc Thach University of Medicine. Ho Chi Minh City, Viet Nam.

**Purpose.** To evaluate the association between ultrasound imaging features and molecular subtypes of breast cancer.

**Materials and methods.** A retrospective study was conducted involving 133 patients with a total of 139 invasive breast carcinoma lesions. All lesions underwent immunohistochemical (IHC) analysis to classify molecular subtypes. Breast ultrasound was performed on all patients prior to biopsy or surgical intervention. The ultrasound images were retrospectively reviewed by two radiologists, each with over five years of experience, who were blinded to the IHC results to ensure statistical independence. Univariate and multivariate logistic regression models were utilized to assess the association between ultrasound characteristics and breast cancer molecular subtypes.

**Results and discussion.** The study analyzed 133 patients diagnosed with breast cancer, among whom 6 presented with two separate tumors, resulting in a total of 139 lesions. These lesions were classified into four molecular subtypes: Luminal A (LA) accounted for 39.6% (n=55), Luminal B (LB) for 36% (n=50), HER2-enriched for 14.4% (n=20), and triple-negative breast cancer (TNBC) represented the smallest proportion at 10% (n=14). Ultrasound imaging features demonstrated significant associations with certain molecular subtypes. Lesions classified as LA were characterized by posterior acoustic shadowing (odds ratio [OR] = 3.0), the presence of echogenic rim (OR = 6.2), and the absence of lymph node metastasis (OR = 4.8). In contrast, HER2-enriched lesions were significantly associated with lymph node metastasis (OR = 4.8), indistinct tumor margins (OR = 15.6), and the presence of microcalcifications (OR = 4.8). TNBC lesions were predominantly associated with posterior acoustic enhancement (OR = 11.4), the absence of microcalcifications (OR = 7.6), and the absence of an echogenic rim (OR = 7.1). No statistically significant correlation was observed between ultrasound features and the LB subtype.

**Conclusion.** The characteristics of margin, posterior acoustic features, microcalcifications, boundary and lymph node status help differentiate between the LA, HER2-enriched and TNBC subtypes.

Keywords: Breast cancer, molecular subtypes, ultrasound, immunohistochemistry.

Corresponding author: Nguyen Duy Hung, e-mail: nguyenduyhung\_84@yahoo.com

*For citation: Tran Thi Hue, Dang Thi Hanh, Le Thi Mai Huong, Nguyen Van Tuan, Nguyen Thu Huong, Nguyen Duy Hung, Nguyen Minh Duc. The value of ultrasound in prediction breast cancer molecular subtypes. REJR 2025; 15(1):95-106. DOI: 10.21569/2222-7415-2025-15-1-95-106.*

Received: 13.02.25

Accepted: 24.02.25

**RUSSIAN ELECTRONIC JOURNAL OF RADIOLOGY**  
**ЭФФЕКТИВНОСТЬ УЛЬТРАЗВУКОВОГО ИССЛЕДОВАНИЯ В ПРОГНОЗИРОВАНИИ**  
**МОЛЕКУЛЯРНЫХ ПОДТИПОВ РАКА МОЛОЧНОЙ ЖЕЛЕЗЫ**

Тран Тхи Хуэ<sup>1,2</sup>, Данг Тхи Хань<sup>2,3</sup>, Ле Тхи Май Хьонг<sup>2</sup>, Нгуен Ван Туан<sup>4</sup>, Нгуен Тху Хьонг<sup>1</sup>,  
Нгуен Зуй Хунг<sup>2,5</sup>, Нгуен Минь Дык<sup>6</sup>

1 – Центр лечения заболеваний молочной железы, Международная больница Винмек Таймс Сити. Ханой, Вьетнам.

2 – Кафедра лучевой диагностики, Ханойский медицинский университет. Ханой, Вьетнам.

3 – Кафедра лучевой диагностики, Генеральная больница Ха Донг. Ханой, Вьетнам.

4 – Центр лучевой диагностики, Больница Ханойского медицинского университета. Ханой, Вьетнам.

5 – Кафедра лучевой диагностики, Больница Вьет Дык. Ханой, Вьетнам.

6 – Кафедра лучевой диагностики, Университет медицины Фам Нгок Тхак. Хошимин, Вьетнам.

**Ц**ель исследования. Оценить взаимоотношения между ультразвуковыми признаками и молекулярными подтипами рака молочной железы.

**Материалы и методы.** Проведено ретроспективное исследование с участием 133 пациенток со 139 очагами инвазивной карциномы молочной железы. Все очаги были подвергнуты иммуногистохимическому (ИГХ) анализу для классификации молекулярных подтипов. Ультразвуковое исследование молочных желез было выполнено всем пациенткам до биопсии или хирургического вмешательства. Ультразвуковые изображения были ретроспективно проанализированы двумя специалистами (врачами ультразвуковой диагностики, каждый с опытом работы более пяти лет), которые не имели доступа к результатам ИГХ для обеспечения статистической независимости. Для оценки взаимосвязи между ультразвуковыми признаками и молекулярными подтипами рака молочной железы использовались однофакторные и многофакторные логистические регрессионные модели.

**Результаты и обсуждение.** В исследовании проанализированы данные 133 пациенток с диагнозом рака молочной железы, среди которых у 6 были выявлены два отдельных опухолевых очага, что в сумме составило 139 очагов. Эти очаги были классифицированы на четыре молекулярных подтипа: Luminal A (LA) – 39,6% (n=55), Luminal B (LB) – 36% (n=50), HER2-позитивный – 14,4% (n=20), трижды негативный рак молочной железы (TNBC) был представлен в наименьшем количестве – 10% (n=14). Ультразвуковые признаки продемонстрировали значимые ассоциации с определенными молекулярными подтипами. Очаги, классифицированные как LA, характеризовались задним акустическим затенением (отношение шансов [ОШ] = 3,0), наличием экзогенного ободка (ОШ = 6,2) и отсутствием метастазов в лимфатических узлах (ОШ = 4,8). В то же время HER2-позитивные очаги были значимо связаны с наличием метастазов в лимфатических узлах (ОШ = 4,8), нечеткими контурами опухоли (ОШ = 15,6) и наличием микрокальцинатов (ОШ = 4,8). Очаги TNBC преимущественно ассоциировались с задним акустическим усилением (ОШ = 11,4), отсутствием микрокальцинатов (ОШ = 7,6) и отсутствием экзогенного ободка (ОШ = 7,1). Статистически значимой корреляции между ультразвуковыми признаками и подтипом LB выявлено не было.

**Заключение.** Характеристики краев опухоли, задние акустические эффекты, наличие микрокальцинатов, границы опухоли и статус лимфатических узлов помогают дифференцировать подтипы LA, HER2-позитивный и TNBC.

Ключевые слова: рак молочной железы, молекулярные подтипы, ультразвук, иммуногистохимия.

Контактный автор: Нгуен Зуй Хунг, e-mail: nguyenduyhung\_84@yahoo.com

Для цитирования: Тран Тхи Хуэ, Данг Тхи Хань, Ле Тхи Май Хьонг, Нгуен Ван Туан, Нгуен Тху Хьонг, Нгуен Зуй Хунг, Нгуен Минь Дык. Эффективность ультразвукового исследования в прогнозировании молекулярных подтипов рака молочной железы. REJR 2025; 15(1):95-106. DOI: 10.21569/2222-7415-2025-15-1-95-106.

Статья получена: 13.02.25

Статья принята: 24.02.25

**B**reast cancer is the most common malignant tumor and is the foremost cause of death in female around the globe [1]. Breast cancer is characterized by diverse molecular profiles, which are classified into four distinct subtypes based on the St. Gallen Consensus 2015: Luminal A (LA), Luminal B (LB), HER2-enriched and triple-negative breast cancer (TNBC). These subtypes are defined by the differential expression of estrogen receptors (ER), progesterone receptors (PR), human epidermal growth factor receptor 2 (HER2), and the proliferation marker Ki67 [2]. Notable variations exist in clinical presentation, imaging findings, treatment approaches, and prognostic outcomes among these molecular subtypes [3-5]. Therefore, accurate preoperative identification of the molecular subtype is crucial for guiding therapeutic strategies and assessing the prognosis of patients.

The classification of molecular subtypes (MS) is determined through gene expression profiling (GEP), first proposed by Perou in 2000 [6]. However, GEP requires advanced techniques, modern equipment, and high costs, which limits its widespread application, especially in countries with limited resources. To address this issue, immune marker profiling (HMMD) has emerged as an alternative method to indirectly assess gene expression through immune markers. Numerous studies have demonstrated that HMMD testing can classify breast cancer MS similarly to genetic analysis [7-9]. However, it remains an invasive diagnostic method, with high costs and lengthy procedures. Therefore, the ability to identify molecular subgroups using non-invasive imaging methods would be advantageous in significantly improving the diagnostic process.

Ultrasound is a non-invasive, cost-effective imaging modality that offers quick results and widespread accessibility. Unlike biopsy, which only samples a portion of the tumor, ultrasound enables the assessment of the entire lesion. Although ultrasound cannot replace genetic testing or histopathological methods, its advantage lies in its ability to provide comprehensive information about the imaging characteristics of the tumor. This makes ultrasound a valuable tool in identifying the features of breast cancer molecular subtypes, thereby enhancing the accuracy of diagnosis and treatment.

Several studies have been conducted indicating that ultrasound has the potential to predict molecular subtypes based on certain tumor characteristics; however, the results have not been consistent [10-13]. Therefore, this study was conducted to provide additional information on the value of ultrasound in predicting

molecular subtypes of breast cancer.

### **Materials and method.**

#### *Patients.*

A retrospective study was conducted on 133 patients with 139 lesions of invasive breast carcinoma who were examined and treated at Vinmec Times City International General Hospital from January 2020 to December 2024. All patients underwent breast ultrasound prior to biopsy or surgery and had complete histopathological data. Exclusion criteria included patients who had ultrasounds performed after diagnostic and therapeutic interventions (biopsy, surgery, neoadjuvant chemotherapy), those with a history of previous breast cancer, patients with incomplete histopathological results, and those without stored ultrasound images in the Picture Archiving and Communication System (PACS). The study was approved by an institutional ethics committee (Ref: 2839/QD-DHYHN dated June 19, 2024).

#### *Data collection.*

Ultrasound images were collected using the 2D LOGIQ S8 ultrasound machine (GE Healthcare, USA) and the Hitachi Arietta 850 (Fujifilm Healthcare, Japan) with a linear probe operating at a frequency of 7-12 MHz. The images of the lesions were stored in the PACS and were independently evaluated by two breast radiologists with at least 5 years of experience, who were unaware of the histopathological results. In cases of discrepancies, the two radiologists would consult to reach a consensus.

Ultrasound characteristics were analyzed based on the American College of Radiology's Breast Imaging Reporting and Data System (ACR BIRADS) version 5, including:

- + Shape: round, oval (fig. 1C), irregular (fig. 1A, 1B, 2B);
- + Orientation: parallel, non-parallel to the skin surface;
- + Margin: circumscribed (fig. 1C), microlobulated, angular/spiculated (fig. 1A, 2A), indistinct (fig. 1B);
- + Echo pattern: hypoechoic, hyperechoic, mixed;
- + Posterior features: shadowing (fig. 1A), indifferent (fig. 2A), enhancement (fig. 1C), combined pattern (fig. 1C);
- + Boundary: abrupt interface, echogenic rim (fig. 1A);
- + Microcalcification: absent, present (fig. 1B, 2B);
- + The presence of possible axillary lymphadenopathy: > 1cm, round shape, loss of hilar structure, cortical thickening;
- + Characteristics of tumor size (in millimeters), tumor location (left breast, right breast), and specific locations within each breast

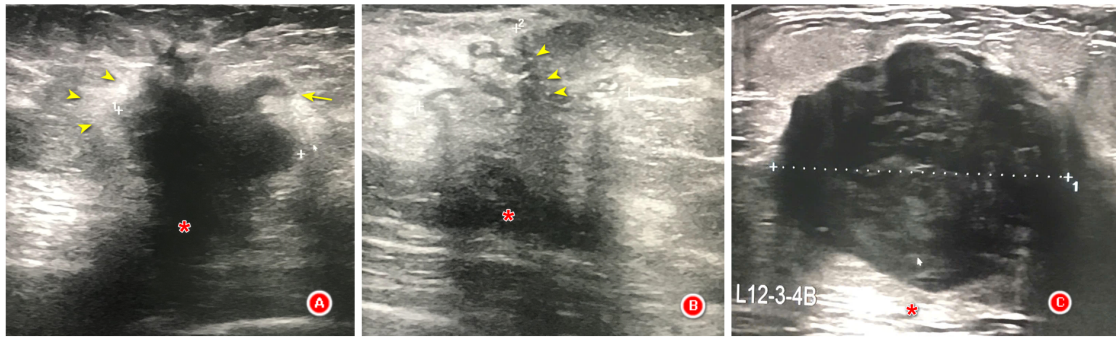


Fig. 1 (Рис. 1)

**Fig. 1. Ultrasound.**

A – LA tumor with irregular shape, spiculated margins (arrow), posterior shadowing (asterisk), echogenic rim sign (arrowhead) and absence of microcalcification.

B – HER2-enriched tumor with irregular shape, indistinct margins, mixed posterior echogenicity (asterisk) and microcalcifications (arrowhead).

C – TNBC tumor with oval shape, posterior enhancement (asterisk), no microcalcifications and no echogenic rim.

**Рис. 1. УЗИ.**

А – Опухоль подтипа Luminal A (LA), с неправильной формой, спикелированными контурами (стрелка), задним акустическим затенением (звездочка), признаком эхогенного ободка (стрелка) и отсутствием микрокальцинатов.

В – Опухоль подтипа HER2-позитивная, с неправильной формой, нечеткими контурами, смешанным задним акустическим эффектом (звездочка) и наличием микрокальцинатов (стрелка).

С – Опухоль подтипа TNBC с овальной формой, с задним акустическим усилением (звездочка), отсутствием микрокальцинатов и эхогенного ободка.

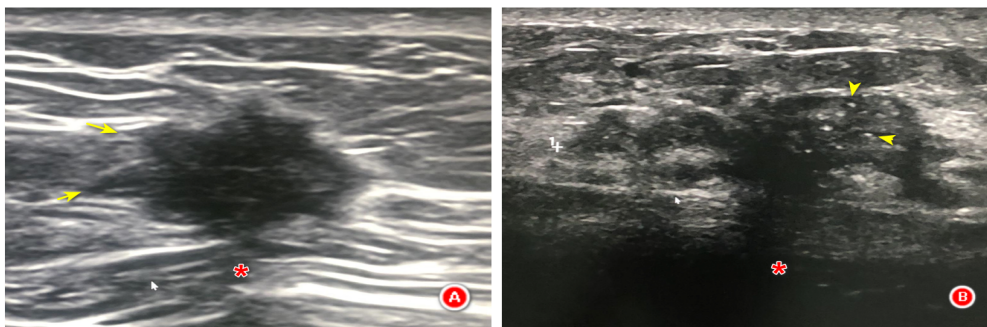


Fig. 2 (Рис. 2)

**Fig. 2. Ultrasound.**

A – LB tumor (HER2 -) has a spiculated margin (arrow), indistinct posterior feature (asterisk) and no microcalcifications.

B – LB tumor (HER2+) has an irregular shape, microcalcifications (arrowhead) and mixed posterior echogenicity (asterisk). However, there is no statistically significant difference with other subtypes.

**Рис. 2. УЗИ.**

А – Опухоль подтипа Luminal B (HER2-негативный), со спикелированными контурами (стрелка), неоднозначным задним акустическим эффектом (звездочка) и отсутствием микрокальцинатов.

В – Опухоль подтипа Luminal B (HER2-позитивный), с неправильной формой, наличием микрокальцинатов (стрелка) и смешанным задним акустическим эффектом (звездочка). Однако статистически значимых различий с другими подтипами не выявлено.



**Table №1. Classification of molecular subtypes according to the St. Gallen 2023 consensus.**

Marker		ER	PR	HER2	Ki-67
Molecular subtypes					
Luminal A		+	+/-	-	Low
Luminal B	HER2 (-)	+	+/-	-	High
	HER2 (+)	+	+/-	+	Hight/low
HER2-enriched		-	-	+	Hight/low
TNBC		-	-	-	Hight/low

**Table №2. Demographic and Pathological Characteristics.**

Characteristics	LA (n=55)	LB (n = 50)	HER2-enriched (n=20)	TNBC (n=14)	P value *	Total
N (%)	55 (39.6%)	50 (36%)	20 (14.4%)	14 (10 %)		139
Age	55.2 ± 13.3	46.1 ± 11.5	50.0 ± 15.2	52.4 ± 12.5	0.005**	
<b>Histological grade</b>						
1	13	1	0	0	0.000 ***	14
2	38	25	13	6		82
3	4	24	7	8		43
<b>Histological type</b>						
IDC#	40	41	20	13	0.036 ***	114
ILC##	5	4	0	0		09
Other types	10	5	0	1		16

\* p-values are calculated by the difference between four subtypes

\*\* ANOVA

\*\*\* G-test (Likelihood Ratio Test)

# Invasive ductal carcinoma

## Invasive lobular carcinoma

(superolateral, superomedial, inferolateral, inferomedial).

*Histopathological and IHC analysis.*

Classification of histopathological type and histological grade according to the World Health Organization (WHO) classification system in 2019<sup>15</sup>.

The expression status of the estrogen receptor (ER), progesterone receptor (PR), and human epidermal growth receptors (HER2) was assessed using the immunohistochemical (IHC) technique. The status of ER and PR was considered positive when more than 1% of tumor cells stained positively. HER2 status was categorized into four levels: 0, 1+, 2+, and 3+, with levels 0 and 1+ considered negative, level 3+ considered positive, and level 2+ classified as ambiguous. Fluorescence in situ hybridization (FISH) was performed on HER2 (2+) tumors to determine the status. In our study, the threshold value for the Ki67 index was set at 20%<sup>16</sup>. The molecular subtypes were classified according to the St. Gallen Consensus 2023<sup>16</sup> (Table №1).

*Statistical Analysis.*

Data were collected using Microsoft Office Excel 2016, and statistical analysis was performed using IBM SPSS version 20. Qualitative variables were tested using Chi-square, Likelihood Ratio Test or Fisher Exact Test, while quantitative variables were tested using T-test or Mann-Whitney U to determine differences in demographic and ultrasound characteristics of the participants. Univariate and multivariate logistic regression analyses were used to estimate the Odds Ratio (OR) and 95% Confidence Interval (CI) for each ultrasound characteristic. Qualitative variables were described by proportions and percentages, while quantitative variables were described by means and standard deviations. Analyses were considered statistically significant when the p-value was less than 0.05.

**Results.**

From January 2020 to November 2024, data were collected from 133 patients diagnosed with invasive breast carcinoma. This cohort included 6 patients with two lesions, while the remaining 127 patients presented with a single lesion each. In total, we identified 139 breast cancer lesions in the study sample, with the LA subtype accounting for 39.6% (n=55), the LB subtype for 36% (n=50), the HER2-enriched subtype for 14.4% (n=20), and the triple-negative breast cancer (TNBC) subtype for 10% (n=14). The demographic and pathological characteristics of the study subjects are presented in Table 2. The average age of the patients in the study was 50.9 ± 13.4 years, ranging from 27 to 83 years. There was a significant difference in age among the patient groups in our study, with a p-value of 0.005. The LA subtype had the highest average

age at 55.2 ± 13.3 years, while the other groups had lower average ages ranging from approximately 46.1 to 52.4 years. Most tumors in the luminal A subtype had low histological grades of I and II, with a rate of 93% (51/55), whereas TNBC tumors predominantly exhibited high histological grade III, accounting for 57% (8/14). This difference was statistically significant with a p-value of 0.000. Regarding histological classification, invasive ductal carcinoma constituted the majority in all subgroups, with rates of 73% (40/55) for LA, 82% (41/50) for LB, 100% for HER2-enriched, and 93% (13/14) for TNBC, while the rates for invasive lobular carcinoma and other types were significantly lower.

Table №3 summarizes the ultrasound imaging characteristics and analyzes the differences in imaging features across the four molecular subtypes. Figures 1 and 2 show ultrasound images of the four subgroups, illustrating the distinct diversity of ultrasound characteristics among the molecular subtypes.

The majority of breast tumors across all four molecular subtypes displayed hypoechoic echogenicity (91%, 127/139) and a parallel orientation relative to the skin surface (84.2%, 117/139), with no statistically significant differences observed among the subtypes. Similarly, no significant variations in tumor size or location were identified across the subtypes, and all imaging features of the LB subtype were comparable to those of the other molecular subtypes.

Tumors in the LA and HER2-enriched subtypes demonstrated significant differences in margin characteristics, posterior acoustic, microcalcifications, boundary and lymph node metastasis compared to the other subtypes. TNBC tumors exhibited distinctive differences in shape, posterior acoustic, microcalcifications and boundary (Table 3).

As presented in Tables №3 and №4, tumors predominantly displayed irregular shapes in the LA subtype (43/55; 78%), LB subtype (34/50; 68%) and HER2-enriched subtype (18/20; 90%) (Figures 1 and 2). Conversely, the majority of TNBC tumors exhibited a round or oval shape, accounting for 64% (9/14) (Figure 1C), demonstrating a statistically significant difference compared to the other subtypes (p = 0.001). Univariate logistic regression analysis further identified a significant association between round or oval shapes and the TNBC subtype, with an odds ratio (OR) of 5.7 and a p-value of 0.003.

Tumors with microlobulated, angular or spiculated margins were predominant, comprising 84% (116/139) of cases. In contrast, only a minor proportion exhibited circumscribed or indistinct margins, accounting for 17% (23/139). Logistic regression analysis demonstrated that the presence of angular or spiculated margins

**Table №3. Sonographic features among four subtypes of breast cancer.**

Parameter	Total n=139	LA (n=55)	LB (n=50)	HER2 – enrich ed (n=20 )	TNBC (n=14 )	<i>p</i> <sup>1</sup>	<i>p</i> <sup>2</sup>	<i>p</i> <sup>3</sup>	<i>p</i> <sup>4</sup>
<b>Tumor size (mm)</b>	17.5 ± 10.5	16.2 ± 10.6	18.2 ± 11.5	18.0 ± 7.2	19.9 ± 11.1	0.098	0.993	0.826	0.220
<b>Location</b>									
Left	75	32	25	11	7	0.419	0.483	0.919	0.754
Right	64	23	25	9	7				
<b>Superolateral</b>	52	18	22	7	5	0.780	0.567	0.983	0.410
<b>Superomedial</b>	36	16	10	5	5				
<b>Inferolateral</b>	21	8	7	3	3				
<b>Inferomedial</b>	30	13	11	5	1				
<b>Shape</b>									
Oval/round	39	12	16	2	9	0.185	0.438	0.052	<b>0.001</b>
Irregular									*
Irregular	100	43	34	18	5				
<b>Orientation</b>									
Parallel	117	43	43	19	13	0.074	0.785	0.309	0.694
Not parallel	22	12	7	1	1				
<b>Margin</b>									
Circumscribed	8	2	3	0	3	<b>0.000</b>	0.116	<b>0.000</b>	0.089
Miclobulated	71	21	32	10	8	*		*	
Angular/spiculated	45	30	12	1	2				
Indistinct	15	2	3	9	1				
<b>Echo pattern</b>									
Hypochoic	127	51	47	18	11	0.272	0.515	0.804	0.214
Hyperechoic	1	1	0	0	0				
Complex	11	3	3	2	3				
<b>Posterior features</b>									

Shadowing	50	34	13	3	0	<b>0.000</b>	0.197	<b>0.013</b>	<b>0.000</b>
Indifferent	23	10	9	3	1	*		*	*
Enhancement	31	7	11	3	10				
Combined pattern	35	4	17	11	3				
<b>Boundary</b>									
Abrupt interface	66	11	28	15	12	<b>0.000</b>	0.132	<b>0.008</b>	<b>0.003</b>
Echogenic rim	73	44	22	5	2	*		*	*
<b>Microcalcification</b>									
Absent	80	39	24	6	12	<b>0,015</b>	0.066	<b>0,006</b>	<b>0.028</b>
Present	59	16	26	14	2	*		*	*
<b>Lymph node status</b>									
Negative	87	43	27	8	9	<b>0.002</b>	0.117	<b>0.024</b>	0.890
Positive	52	12	23	12	5	*		*	

\* Result with statistically significant difference  $p < 0,05$

<sup>1</sup>p value calculated the difference between LA vs other

<sup>2</sup>p value calculated the difference between LB vs other

<sup>3</sup>p value calculated the difference between enriched HER2 vs other

<sup>4</sup>p value calculated the difference between TNBC vs other

The values  $p^1$ ,  $p^2$ ,  $p^3$ ,  $p^4$  are tested by Independent Samples T-test, Mann-Whitney U, Chi-squared ( $\chi^2$ ), Likelihood Ratio Test or Fisher Exact Test

significantly increased the likelihood of a LA subtype (univariate: OR = 5.5,  $p < 0.001$ ) (fig. 1A). Additionally, indistinct margins were associated with a higher probability of HER2-enriched subtype (univariate: OR = 15.4,  $p < 0.001$ ; multivariate: OR = 13.5,  $p = 0.002$ ) (fig. 1B).

Regarding posterior wall echo characteristics, tumors with posterior acoustic enhancement were mainly found in the TNBC subgroup (10/14, 71%) compared to the remaining tumors (fig. 1C), which was a strong predictor for TNBC (univariate: OR = 12.4 and  $p = 0.000$ , multivariate: OR = 8.2 and  $p = 0.005$ ). A mixed-echo pattern was common in HER2-enriched tumors (11/20, 55%) (fig. 1B) and was associated with HER2 after univariate analysis (OR = 4.8,  $p = 0.002$ ). In contrast, posterior wall echo was more common in LA (34/55, 62%) (fig. 1A), which was confirmed in univariate logistic regression with

OR = 6.9,  $p = 0.000$  and multivariate with OR = 2.9,  $p = 0.040$ .

Tumor microcalcifications characteristic were common in the HER-enriched subgroup (14/20, 70%) (fig. 1B). Logistic regression showed that the presence of microcalcifications was associated with HER2 (univariate: OR = 3.8,  $p = 0.010$ ; multivariate: OR = 3.7,  $p = 0.039$ ), while the absence of microcalcifications was associated with LA (univariate: OR = 2.6,  $p = 0.11$ ) and TNBC (univariate: OR = 4.9,  $p = 0.044$ , multivariate: OR = 7.6,  $p = 0.022$ ).

Tumors belonging to the LA subtype were more likely to have a surrounding echogenic halo (44/55, 80%) than the remaining tumors ( $p = 0.000$ ) (fig. 1 A). The presence of a halo increased the likelihood of having the LA subtype (univariate: OR = 7.6,  $p = 0.000$ ; multivariate: OR = 6.2,  $p = 0.000$ ), while the absence of a surrounding



**Table №4. Univariate and multivariate logistic regression analysis.**

Subtype	Univariate logistic regression analysis			Multivariate logistic regression analysis		
	Predictive SS	OR 95%CI	<i>P</i> value	Independent predictors	OR 95%CI	<i>P</i> value
<b>LA</b>	Angular/spiculated margin	5.5 2.6 – 11.9	0.000	-	-	-
	Posterior shadowing	6.9 3.2 – 14.9	0.000	Posterior shadowing	3.0 1.1 – 8.4	0.039
	No microcalcifications	2.4 1.2 – 5.0	0.011	-	-	-
	Echogenic rim sign	7.6 3.4 – 16.7	0,000	Echogenic rim sign	6.2 2.2 – 17.2	0.000
	No lymph node	3.3 1.5 – 7.0	0.003	No lymph node	4.8 1.8 – 12.5	0.002
<b>HER2-enriched</b>	Indistinct margin	15.4 4.6 – 51.4	0,000	Indistinct margin	15.6 3.6 – 67.6	0,000
	Mixed posterior echogenicity	4.8 1.8 – 13.0	0,002	-	-	-
	Microcalcification	4.0 1.4 – 11.1	0,010	Microcalcification	4.8 1.3 – 17.1	0.015
	Abrupt interface	4.0 1.4 – 11.7	0.012	-	-	-
	Lymph node metastasis	2.9 1.1 – 7.8	0.029	Lymph node metastasis	4.8 1.4 – 16.6	0.014
<b>TNBC</b>	Round/oval	5.7 1.8 – 18.3	0.003	-	-	-
	Posterior enhancement	12.4 3.5 – 43.2	0.000	Posterior enhancement	11.4 2.3 – 57.5	0.003
	No microcalcification	4.9 1.05 – 22.7	0.044	No microcalcification	7.6 1.3 – 42.9	0.022
	Abrupt interface	7.9 1.7 – 36.7	0.008	Abrupt interface	7.1 1.2 – 41.1	0.030

halo was associated with the LB subtype in univariate analysis (OR = 4.0,  $p = 0.012$ ).

Lymph node metastasis status was also significant in predicting DNPT, with lymph node metastasis predicting HER2-enriched subgroup (univariate: OR = 2.9,  $p = 0.029$ ; multivariate: OR = 4.5,  $p = 0.017$ ), without lymph node metastasis predicting LA subgroup (univariate: OR = 3.3,  $p = 0.003$ , multivariate: OR = 4.7,  $p = 0.002$ ).

#### Discussion.

This study aimed to investigate the correlation between ultrasound imaging features and breast cancer subtypes. Through a detailed analysis of the ultrasound characteristics of invasive breast carcinoma across different molecular subtypes, significant variations were identified among the subtypes. These findings enhance the understanding of the imaging profiles associated with each subtype and underscore the potential role of ultrasound as a valuable adjunct in subtype classification, supporting clinicians in both diagnosis and treatment planning.

We observed a statistically significant association between the presence of posterior acoustic shadowing, echogenic rim and the absence of lymph node metastasis in the LA subtype, with  $p$ -values of 0.039, 0.000 and 0.002, respectively. These findings are consistent with prior studies [10,11,17,18]. The phenomenon of desmoplastic reaction has been noted in previous research, tumors within this subtype typically exhibit low histological grades and slow growth, which stimulate a fibrous tissue response surrounding the tumor, leading to the formation of spiculated margins and a surrounding echogenic rim. This reactive area also contributes to the acoustic shadowing observed behind the lesion [10, 19]. Moreover, the absence of lymph node metastasis reflects the less invasive nature of the LA subtype, a characteristic also confirmed in Khalaf's study, which identified lymph node metastasis as an independent predictive factor for the HER2-enriched subtype when present and for the LA subtype when absent [11].

For the HER2-enriched subtype, the characteristics of indistinct margin ( $p = 0.00$ ), microcalcifications ( $p = 0.015$ ) and the presence of lymph node metastasis ( $p = 0.014$ ) were identified as independent predictive factors. HER2-enriched tumors frequently exhibit indistinct margins, which aligns with the findings of Tong Wu10. The presence of microcalcifications is closely associated with HER2 overexpression, a feature documented in several prior studies [10-13, 17, 20, 21]. This correlation can be attributed to the common occurrence of ductal carcinoma in situ (DCIS) accompanying HER2-enriched tumors, as DCIS is known to be associated with microcalcifications [12, 22, 23]. In contrast to the LA subtype, tumors in the HER2-enriched

subtype typically show lymph node metastasis, which is a distinct characteristic reflecting the aggressive nature of HER2-enriched tumors.

TNBC is recognized as the most aggressive subtype of breast cancer with the poorest prognosis. However, numerous studies have demonstrated that TNBC tumors can exhibit benign-like characteristics, such as round or oval shapes, well-defined margins, posterior acoustic enhancement and the absence of microcalcifications [11, 13, 18, 20, 22, 24, 25]. These features can lead to false-negative diagnoses, highlighting the necessity for a more comprehensive understanding of the imaging characteristics of this subtype to prevent oversight during screening and diagnosis. Our study identified characteristics including posterior acoustic enhancement ( $p = 0.003$ ), absence of microcalcifications ( $p = 0.022$ ), and lack of echogenic rim ( $p = 0.030$ ) as predictive factors for TNBC after multivariate logistic regression analysis. Posterior acoustic enhancement observed in TNBC tumors is thought to arise from their high histological grade and rapid proliferation, which frequently leads to necrosis within the tumor. This necrotic tissue allows sound waves to traverse with minimal attenuation. In contrast to LA tumors, which typically exhibit echogenic rim, TNBC tumors in our study predominantly lacked this characteristic, aligning with findings from multiple prior studies, this absence of echogenic rim can be explained by the aggressive and rapid cellular proliferation of TNBC tumors, resulting in compression of surrounding tissues without eliciting a desmoplastic reaction [10, 22, 26]. Conversely, microcalcifications are often associated with HER2-enriched tumors, while TNBC tumors usually do not present with microcalcifications, likely due to the lower incidence of coexisting DCIS [23].

Several previous studies have indicated that tumors classified as LB may exhibit irregular shapes, lack of echogenic rim, indistinct margins or posterior acoustic shadowing [11, 13, 17]. However, our study did not identify any ultrasound features with statistically significant predictive value for the LB subtype. This may be attributed to an insufficient sample size or variability in HER2 expression among tumors within this subtype, leading to differences in imaging characteristics and reducing the ability to distinctly differentiate them from other subtypes.

Our study has certain limitations. First, it is a retrospective analysis conducted at a single medical facility. Second, the relatively small sample size, particularly for the HER2-enriched and TNBC subgroups, may have resulted in insufficient statistical power to detect differences. Third, the study focused solely on ultrasound characteristics, which may have led to the

oversight of discrete microcalcifications, a feature more readily identified on mammography. Therefore, further multicenter studies with larger sample sizes are needed to validate the generalizability of these ultrasound characteristics and to integrate them with other imaging modalities to enhance diagnostic accuracy.

**Conclusion.**

The characteristics of margin, posterior acoustic features, boundary, microcalcifications and lymph node metastasis are closely related to the prediction of LA, HER2-enriched and TNBC subtypes. Understanding these correlations provides clinicians with valuable information for patient classification, which can enhance diagnostic accuracy, treatment strategies, and overall management of breast cancer patients from the outset.

**Ethical approval**

Hanoi Medical University's institutional review board supported this retrospective study (2839/QD-DHYHN dated June 19, 2024). This study was conducted according to the ethical standards of the 1964 Declaration of Helsinki

and its later amendments.

**Informed consent**

The requirement for informed consent was waived.

**Patient consent for publication**

Not applicable.

**Availability of data and material**

The datasets generated and/or analyzed during the current study are not publicly available due to privacy concerns but are available from the corresponding author upon reasonable request.

**Author's contributions**

NDH and NMD wrote the manuscript. All authors participated in the design of the study. All authors were involved in the acquisition of data. All authors participated in the analysis and interpretation of data. TTH and NDH confirmed the authenticity of all the raw data. All authors have read and approved the final manuscript.

**Conflicts of interest**

The authors declare no conflict of interest.

**Funding**

This research received no external funding.

**References:**

1. Bray F, Laversanne M, Sung H, et al. Global cancer statistics 2022: GLOBOCAN estimates of incidence and mortality worldwide for 36 cancers in 185 countries. *CA Cancer J Clin.* 2024;74(3):229-263. doi:10.3322/caac.21834
2. Jackisch C, Harbeck N, Huober J, et al. 14th St. Gallen International Breast Cancer Conference 2015: Evidence, Controversies, Consensus - Primary Therapy of Early Breast Cancer: Opinions Expressed by German Experts. *Breast Care Basel Switz.* 2015;10(3):211-219. doi:10.1159/000433590
3. Sotiriou C, Neo SY, McShane LM, et al. Breast cancer classification and prognosis based on gene expression profiles from a population-based study. *Proc Natl Acad Sci U S A.* 2003;100(18):10393-10398. doi:10.1073/pnas.1732912100
4. Dawood S, Hu R, Homes MD, et al. Defining breast cancer prognosis based on molecular phenotypes: results from a large cohort study. *Breast Cancer Res Treat.* 2011;126(1):185-192. doi:10.1007/s10549-010-1113-7
5. Barzaman K, Karami J, Zarei Z, et al. Breast cancer: Biology, biomarkers, and treatments. *Int Immunopharmacol.* 2020;84:106535. doi:10.1016/j.intimp.2020.106535
6. Perou CM, Sørlie T, Eisen MB, et al. Molecular portraits of human breast tumours. *Nature.* 2000;406(6797):747-752. doi:10.1038/35021093
7. Brenton JD, Carey LA, Ahmed AA, Caldas C. Molecular classification and molecular forecasting of breast cancer: ready for clinical application? *J Clin Oncol Off J Am Soc Clin Oncol.* 2005;23(29):7350-7360. doi:10.1200/JCO.2005.03.3845
8. Tang P, Wang J, Bourne P. Molecular classifications of breast carcinoma with similar terminology and different definitions: are they the same? *Hum Pathol.* 2008;39(4):506-513. doi:10.1016/j.humpath.2007.09.005
9. Nielsen T.O, Hsu F.D, Jensen K, et al (2004). Immunohistochemical and clinical characterization of the basal-like subtype of invasive breast carcinoma. *Clin Cancer Res,* 10, 5367-74.
10. Wu T, Li J, Wang D, et al. Identification of a correlation between the sonographic appearance and molecular subtype of invasive breast cancer: A review of 311 cases. *Clin Imaging.* 2019;53:179-185. doi:10.1016/j.clinimag.2018.10.020
11. Khalaf LMR, Herdan RA. Role of ultrasound in predicting the molecular subtypes of invasive breast ductal carcinoma. *Egypt J Radiol Nucl Med.* 2020;51(1):138. doi:10.1186/s43055-020-00240-z
12. Ian TWM, Tan EY, Chotai N. Role of mammogram and ultrasound imaging in predicting breast cancer subtypes in screening and symptomatic patients. *World J Clin Oncol.* 2021;12(9):808-822. doi:10.5306/wjco.v12.i9.808
13. Rashmi S, Kamala S, Murthy SS, Kotha S, Rao YS, Chaudhary KV. Predicting the molecular subtype of breast cancer based on mammography and ultrasound findings. *Indian J Radiol Imaging.* 2018;28(3):354-361. doi:10.4103/ijri.IJRI\_78\_18
14. Breast Imaging Reporting & Data System | American College of Radiology. Accessed January 6, 2025. <https://www.acr.org/Clinical-Resources/Reporting-and-Data-Systems/Bi-Rads>
15. The 2019 World Health Organization classification of tumours of the breast - Tan - 2020 - Histopathology - Wiley Online Library. Accessed January 9, 2025. <https://onlinelibrary.wiley.com/doi/10.1111/his.14091>
16. Curigliano G, Burstein HJ, Gnani M, et al. Understanding breast cancer complexity to improve patient outcomes: The St Gallen International Consensus Conference for the Primary Therapy of Individuals with Early Breast Cancer 2023. *Ann Oncol Off J Eur Soc Med Oncol.* 2023;34(11):970-986. doi:10.1016/j.annonc.2023.08.017
17. Zhang L, Li J, Xiao Y, et al. Identifying ultrasound and clinical features of breast cancer molecular subtypes by ensemble decision. *Sci Rep.* 2015;5:11085. doi:10.1038/srep11085

18. Shaikh S, Rasheed A. Predicting Molecular Subtypes of Breast Cancer with Mammography and Ultrasound Findings: Introduction of Sono-Mammometry Score. *Radiol Res Pract.* 2021;2021:6691958. doi:10.1155/2021/6691958
19. Çelebi F, Pilancı KN, Ordu Ç, et al. The role of ultrasonographic findings to predict molecular subtype, histologic grade, and hormone receptor status of breast cancer. *Diagn Interv Radiol Ank Turk.* 2015;21(6):448-453. doi:10.5152/dir.2015.14515
20. Huang J, Lin Q, Cui C, et al. Correlation between imaging features and molecular subtypes of breast cancer in young women ( $\leq 30$  years old). *Jpn J Radiol.* 2020;38(11):1062-1074. doi:10.1007/s11604-020-01001-8
21. Ko ES, Lee BH, Kim HA, Noh WC, Kim MS, Lee SA. Triple-negative breast cancer: correlation between imaging and pathological findings. *Eur Radiol.* 2010;20(5):1111-1117. doi:10.1007/s00330-009-1656-3
22. Liao N, Zhang G chun, Liu Y hui, et al. HER2-positive status is an independent predictor for coexisting invasion of ductal carcinoma in situ of the breast presenting extensive DCIS component. *Pathol Res Pract.* 2011;207(1):1-7. doi:10.1016/j.prp.2010.08.005
23. Yang WT, Tse GMK, Lam PKW, Metreweli C, Chang J. Correlation Between Color Power Doppler Sonographic Measurement of Breast Tumor Vasculature and Immunohistochemical Analysis of Microvessel Density for the Quantitation of Angiogenesis. *J Ultrasound Med.* 2002;21(11):1227-1235. doi:10.7863/jum.2002.21.11.1227
24. Panta OB, Dhakal V, Gurung B, Ghimire RK. Correlation of Imaging Findings with Molecular Subtypes of Breast Cancer. *J Nepal Health Res Counc.* 2023;21(1):71-75. doi:10.33314/jnhrc.v21i1.4518
25. Lohitvisate W, Pummee N, Kwankua A. Mammographic and ultrasonographic features of triple-negative breast cancer compared with non-triple-negative breast cancer. *J Ultrasound.* 2022;26(1):193-200. doi:10.1007/s40477-022-00709-9
26. Wojcinski S, Soliman AA, Schmidt J, Makowski L, Degenhardt F, Hillemanns P. Sonographic features of triple-negative and non-triple-negative breast cancer. *J Ultrasound Med Off J Am Inst Ultrasound Med.* 2012;31(10):1531-1541. doi:10.7863/jum.2012.31.10.1531